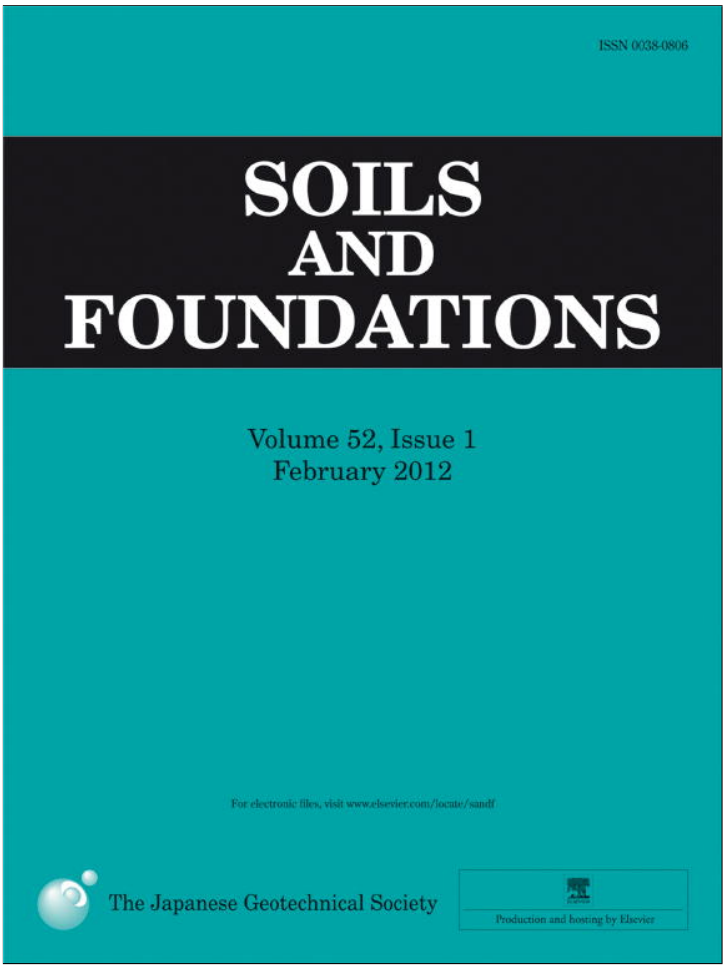
Provided for non-commercial research and education use.
Not for reproduction, distribution or commercial use.



This article appeared in a journal published by Elsevier. The attached copy is furnished to the author for internal non-commercial research and education use, including for instruction at the authors institution and sharing with colleagues.

Other uses, including reproduction and distribution, or selling or licensing copies, or posting to personal, institutional or third party websites are prohibited.

In most cases authors are permitted to post their version of the article (e.g. in Word or Tex form) to their personal website or institutional repository. Authors requiring further information regarding Elsevier's archiving and manuscript policies are encouraged to visit:

http://www.elsevier.com/copyright

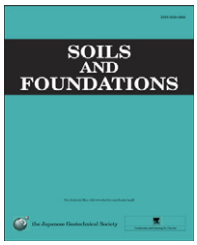
Author's personal copy

Soils and Foundations 2012;52(1):69–80

The Japanese Geotechnical Society

Soils and Foundations

www.sciencedirect.com
journal homepage: www.elsevier.com/locate/sandf



Prediction of bearing capacity of circular footings on soft clay stabilized with granular soil

Murat Ornek[a], Mustafa Laman[b,*], Ahmet Demir[c], Abdulazim Yildiz[d]

[a]*Mustafa Kemal University, Civil Engineering Department, 31200 Iskenderun, Hatay, Turkey*
[b]*Adana Science and Technology University, Civil Engineering Department, Adana, Turkey*
[c]*Osmaniye Korkut Ata University, Civil Engineering Department, 80000 Osmaniye, Turkey*
[d]*Cukurova University, Civil Engineering Department, 01330 Balcali, Adana, Turkey*

Available online 2 February 2012

Abstract

The shortage of available and suitable construction sites in city centres has led to the increased use of problematic areas, where the bearing capacity of the underlying deposits is very low. The reinforcement of these problematic soils with granular fill layers is one of the soil improvement techniques that are widely used. Problematic soil behaviour can be improved by totally or partially replacing the inadequate soils with layers of compacted granular fill. The study presented herein describes the use of artificial neural networks (ANNs), and the multi-linear regression model (MLR) to predict the bearing capacity of circular shallow footings supported by layers of compacted granular fill over natural clay soil. The data used in running the network models have been obtained from an extensive series of field tests, including large-scale footing diameters. The field tests were performed using seven different footing diameters, up to 0.90 m, and three different granular fill layer thicknesses. The results indicate that the use of granular fill layers over natural clay soil has a considerable effect on the bearing capacity characteristics and that the ANN model serves as a simple and reliable tool for predicting the bearing capacity of circular footings in stabilized natural clay soil.
© 2012. The Japanese Geotechnical Society. Production and hosting by Elsevier B.V. All rights reserved.

Keywords: Bearing capacity; Clay; Field test; Footing; Granular material; Load test; Neural networks

1. Introduction

Recently, there is an increasing demand to construct on soft subsoils, which were considered unsuitable for construction in the past. Soft soils, such as normally consolidated or slightly overconsolidated clays, have high compressibility and low shear strength. They include a variety of materials such as loose silts, clays, organic soils and peat. These materials can be found throughout the world. Shallow footings, when built on these soils, have a low load-bearing capacity and undergo large settlements. Construction on soft soils often requires the utilisation of ground improvement techniques. Reinforcement of the soft soils with granular fill layers is a soil improvement technique that is widely used. Soft soil behaviour can be improved by totally or partially replacing the inadequate soils with layers of compacted granular fill.

*Corresponding author. Tel./fax: +90 322 338 67 02.
E-mail addresses: mornek@mku.edu.tr (M. Ornek), mlaman@cukurova.edu.tr (M. Laman), ahmetdemir@osmaniye.edu.tr (A. Demir), azim@cukurova.edu.tr (A. Yildiz).

0038-0806 © 2012. The Japanese Geotechnical Society. Production and hosting by Elsevier B.V. All rights reserved.

Peer review under responsibility of The Japanese Geotechnical Society
doi:10.1016/j.sandf.2012.01.002



Production and hosting by Elsevier

Author's personal copy

Physical modelling can be carried out through either a full-scale model or a small-scale model in geotechnical engineering. Full-scale modelling is generally performed with the real-site conditions, such as the ground conditions, loads and stress levels. Hence, the results obtained from this type of modelling are more accurate than those from other types of modelling. Despite their operational and financial disadvantages, large- and full-scale field tests produce more reasonable results when simulating the soil behaviour and modelling a geotechnical structure. Large-scale field tests were conducted in this study to overcome the shortcomings of small-scale laboratory model tests and to more accurately model the full-scale behaviour of reinforced soil footings.

Several experimental and numerical studies have been described for the reinforcement of weak soft soils (Ochiai et al., 1996; Adams and Collin, 1997; Yin, 1997; Otani et al., 1998; Alawaji, 2001; Dash et al., 2003; Thome et al., 2005; Chen, 2007; Deb et al., 2007). Ochiai et al. (1996) summarised the theory and practice of the geosynthetic reinforcement of fills over extremely soft grounds in Japan. Adams and Collin (1997) conducted 34 large-model load tests to evaluate the potential benefits of geosynthetic-reinforced spread foundations. It was concluded that the soil-geosynthetic system formed a composite material that inhibited the development of the soil-failure wedge beneath shallow spread foundations. Otani et al. (1998) studied the behaviour of a strip foundation constructed on reinforced clay. The settlement was found to be reduced by increasing the reinforcement size, the stiffness and the number of layers. The load-carrying capacity of foundations has been found to increase more on soil in which reinforcements are provided at closer spacing. Alawaji (2001) discussed the effects of reinforcing sand pads over collapsible soil and reported that a successive reduction in collapse settlement, up to 75%, was obtained. Dash et al. (2003) performed model tests in the laboratory to study the response of reinforcing granular fill overlying soft clay beds and showed that substantial improvements in the load-carrying capacity and a reduction in surface heaving of the foundation bed were achieved.

Artificial neural networks are a form of artificial intelligence; they try to simulate the behaviour of the human brain and nervous system. They have the ability to relate the input data and the corresponding output data, which can be defined depending on the single or multiple parameters employed to solve the linear or nonlinear problems. In recent years, the use of artificial neural networks has increased in geotechnical engineering. Artificial neural networks have been successfully applied to many geotechnical engineering problems, such as pile capacity, settlement of foundations, soil properties and behaviour, liquefaction, earth-retaining structures, slope stability, tunnels and underground openings. Comprehensive information on the above-mentioned applications can be found in the literature (Fausett, 1994; Nawari et al., 1999; Wang and Rahman, 1999; Shahin et al., 2001; Juang et al., 2001; Basma and Kallas, 2004; Kung et al., 2007; Cobaner et al., 2008; Kayadelen, 2008; Kuo et al., 2009; Padmini et al., 2008; Cho, 2009; Laman and Uncuoglu, 2009; Samui, 2010).

The study presented herein describes the use of artificial neural networks (ANNs) and the multi-linear regression model (MLR) to predict the bearing capacity of circular shallow footings supported by layers of compacted granular fill over natural clay soil. The data used to run the network models have been obtained from an extensive series of field tests, including large-scale footing diameters. The field tests were performed using seven different footing diameters, up to 0.90 m, and three different granular fill layer thicknesses. The large-scale testing was performed at the Adana Metropolitan Municipality's (AMM) Water Treatment Facility Centre (WTFC) located in the western part of Adana, Turkey. A total of 28 tests were conducted using a model footing with diameters of 0.06, 0.09, 0.12, 0.30, 0.45, 0.60 and 0.90 m. The primary objectives of these large-scale experiments were to model the full-scale behaviour of reinforced soil footings more accurately, to evaluate the performance of granular fill layers stabilizing the natural clay soil, with respect to the bearing capacity, and to examine the effects of the thickness of granular fill layers. To the best of the authors' knowledge, the effect of granular fill layers on the bearing capacity behaviour of large-scale footings on natural clay deposits and the statistical support with artificial intelligence have not yet been investigated in foundation engineering.

2. Field tests

It is known from the literature that most of the experimental studies on reinforced soils were conducted using small-scale laboratory tests. Due to the scale effect, it is sometimes difficult to accurately model the full-scale behaviour of reinforced soil in small-scale laboratory tests (Abu-Farsakh et al., 2008). For this reason, large-scale field tests were conducted on natural clay deposits and layers of compacted granular fill overlying natural clay deposits.

2.1. Site characterization

A total of 28 field tests were conducted in the Adana Metropolitan Municipality's (AMM) Water Treatment Facility Center (WTFC) located in the western part of Adana, Turkey. The soil conditions at the experimental test site (WTFC) were determined from a geotechnical site investigation comprising both field and laboratory tests. Two test pit excavations (TP1 and TP2) and four borehole drillings (BH1, BH2, BH3 and BH4) were performed in the WTFC test area (Fig. 1). The test area had dimensions of 30 m (length) by 11.6 m (width). Test pits of 2.50 m were excavated and boreholes were drilled with diameters of 0.10 m and depths of 13 m. The borehole drilled on the south side was 20 m. The ground water level was observed as being 2.20 m from the borehole drillings. The saturation ratio of the clay layer, where the tests were conducted, was about 80%. Three subsoil layers were clearly identified by visual inspection and by the Unified Soil Classification System (USCS). The first layer, 0.80 m in depth, was

Author's personal copy

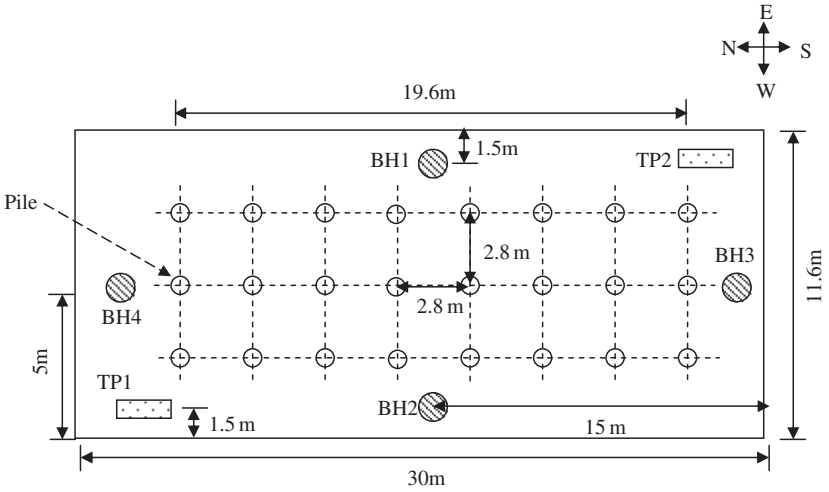


Fig. 1. Plan view showing piles, borings and test pits.

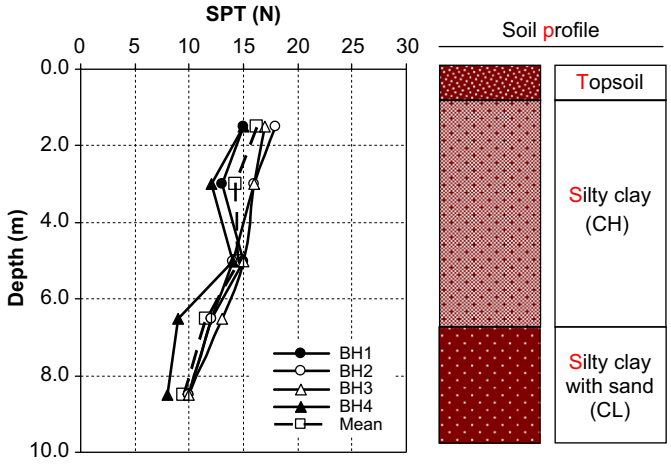


Fig. 2. SPT(N) values measured from boreholes.

observed as topsoil and was removed before the tests. The intermediate layer, between the depths of 0.80 m and 7.0 m, exhibited a silty clay stratum with high plasticity (CH). A silty clay layer, with the intrusion of sand (CL), was observed in the bottom layer to a depth of 10.0 m. Standard Penetration Tests (SPT) were carried out during the drilling of each borehole, and the distribution of SPT values with depth is shown in Fig. 2. These values infer that the tested soil was classified as medium stiff clay. Conventional laboratory tests, such as sieve analysis, moisture content, Atterberg limit, specific gravity, standard proctor, unconfined compression, laboratory vane, triaxial and consolidation tests, were performed in the Geotechnical Laboratory of the Civil Engineering Department at Cukurova University, Adana, Turkey. The clay content of the soil layers varied from 60% to 70%. The upper homogeneous layer, where all the loading tests were carried out, was classified as high plasticity clay (CH) according to USCS. The water content of the stratified soil layers varied between 20% and 25%, depending on depth, which was almost the same as, or greater than, the plastic limit. The specific gravities of the soil layers (G_s) varied from 2.60 to 2.65 along the depths. The values of the undrained shear strengths, c_u, were determined by unconfined compression tests in the range of 60–80 kN/m^2. The average value of undrained shear strength from the triaxial tests was obtained as 65 kN/m^2. The soil layers were classified as lightly overconsolidated soil (OCR = 1–2.65) from odometer tests. The clay content, the water content and the unconfined strength of the natural clay deposits along the depths are presented in Fig. 3. Triaxial, consolidation and unconfined compression tests were conducted on undisturbed soil samples derived from the field.

2.2. Details of model footings and granular fill material used

Seven different footings with diameters of 0.06, 0.09, 0.12, 0.30, 0.45, 0.60 and 0.90 m were used in this study. These rigid, steel footings had thicknesses of 0.02 m for $D \leq 0.12$ m and 0.03 m for $D > 0.12$ m, where D is the footing diameter. The granular fill material used in the model tests was obtained from the Kabasakal region situated northwest of Adana, Turkey. Some conventional tests (sieve analysis, moisture content, unit weight, direct shear and proctor tests) were conducted on this material. The granular soil was prepared at the optimum moisture content value of 7% and a maximum dry unit weight of 21.7 kN/m^3 obtained from standard proctor tests (Fig. 4(b)). The values for the internal friction angle and the cohesion of granular fill were obtained as 43° and 15 kN/m^2, respectively, from direct shear tests. The square-shaped direct shear box had a width of 60 mm. The specific gravity of the granular soil was obtained as 2.64. From the sieve analysis, the granular soil was classified as well-graded gravel-silty gravel, GW-GM, according to USCS. Fig. 4(a) shows the particle size distribution of the natural granular fill material. However, the granular fill material used in the laboratory conventional and field tests was obtained by passing natural granular material through a sieve with 4.75-mm openings. The reason was to provide homogeneity in the laboratory and field test conditions.

Author's personal copy

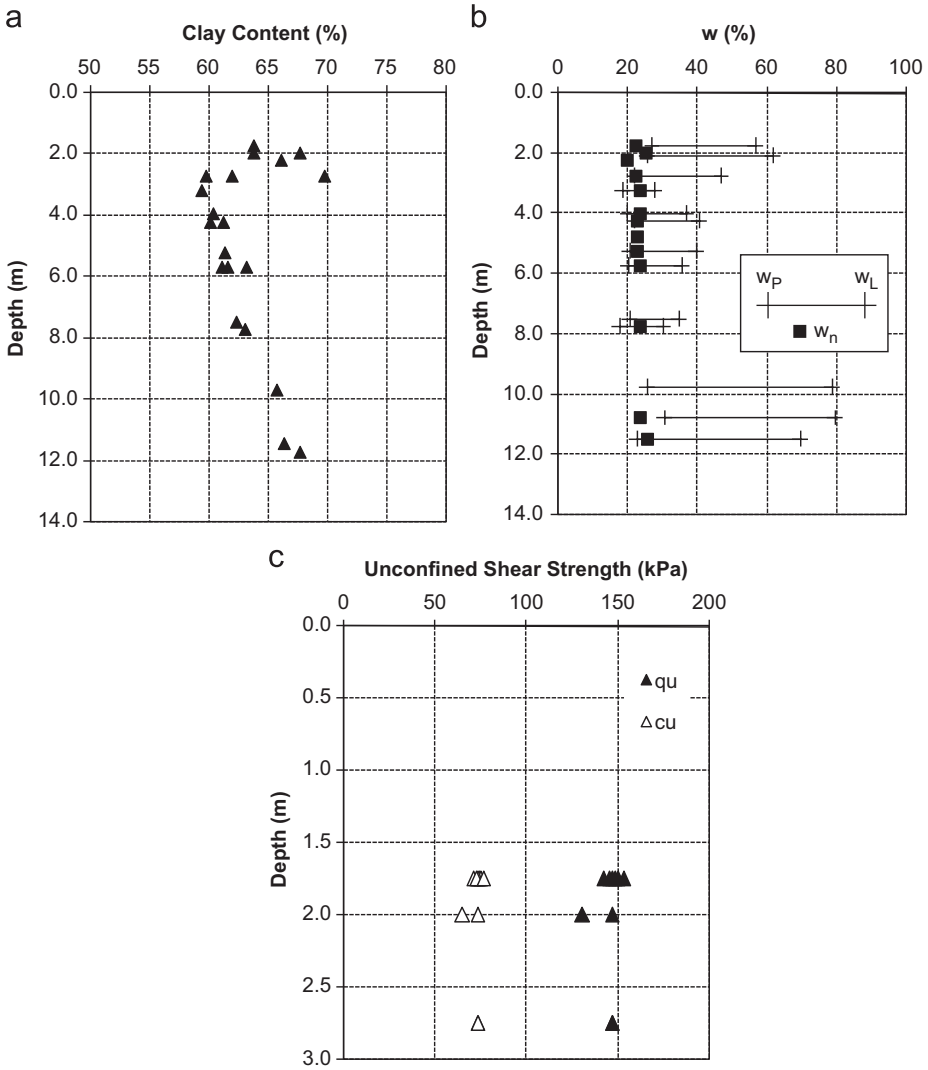


Fig. 3. Distribution of typical soil characteristics of natural clay soil. (a) Clay content, (b) Water content and (c) Shear strength.

2.3. Experimental set-up and test programme

After obtaining the soil properties of the WTFC test area, 24 piles were constructed. The topsoil was removed before the tests. Then, reaction piles were connected with a steel beam. The top surface of the test area was leveled, and the footing was placed on a predefined alignment such that the loads from the hydraulic jack and the loading frame would be transferred concentrically to the footing. A hydraulic jack against the steel beam provided downward load. The hydraulic jack and the two linear variable displacement transducers (LVDT) were connected to a data logger unit and the data logger unit was connected to a computer. The granular fill material was placed and compacted in layers. The thickness of each layer was changed depending on the footing diameter. The amounts of granular fill material and water needed for each layer were firstly calculated. Then, the granular fill material was compacted using a plate compactor to a predetermined height to achieve the desired density. The compacted granular fill layer had a moisture content of 7% and a unit weight of 20.20 kN/m^3. Load was applied with a hydraulic jack and maintained manually with a hand pump. The load and the corresponding footing settlement were measured with a calibrated pressure gauge and two LVDTs, respectively. The testing procedure was performed according to ASTM D 1196-93 (ASTM, 1997), where the load increments were applied and maintained until the rate of the settlement was less than 0.03 mm/min over three consecutive minutes.

Some tests were repeated twice to verify the repeatability and the consistency of the test data. The same pattern for the load–settlement relationship, with a difference in ultimate load values of less than 2.0%, was obtained. The difference was considered to be small, and thus, ignored. The tests were continued until the applied vertical load was clearly reduced or a considerable settlement of the footing was obtained from a relatively small increase in vertical

Author's personal copy

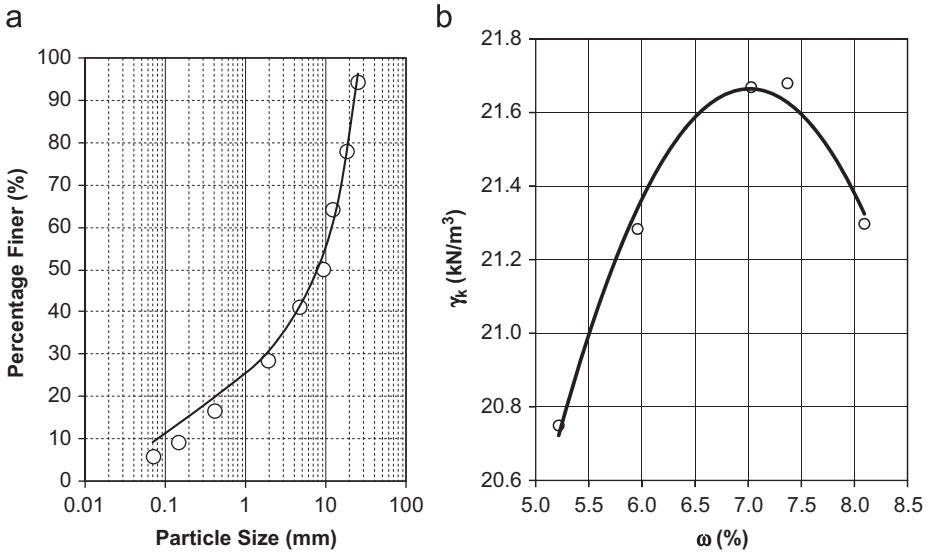


Fig. 4. Typical soil characteristics of granular fill material. (a) Particle Size Distribution (Natural Granular Material) and (b) Optimum Moisture Content.

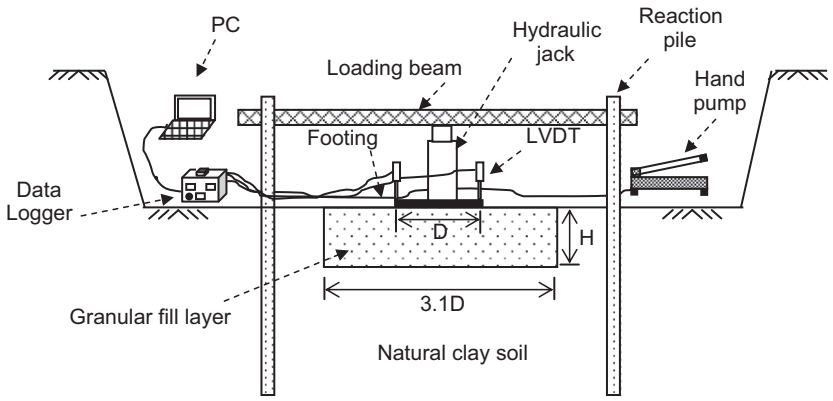


Fig. 5. Schematic view of test set-up, loading, reaction system and typical layout of instrumentation.

load. Detailed information on the testing procedure can be found by Laman et al. (2009) and Ornek (2009). The general layout of the test set-up is given in Fig. 5.

The research was conducted in two series. Series I consisted of tests with seven different footing diameters (0.06, 0.09, 0.12, 0.30, 0.45, 0.60 and 0.90 m) on the surface of the natural clay deposit. Series II was the same as Series I, except that the footings were placed on the granular fill layers settled on the natural clay deposit. The granular fill layers were designed in three different thicknesses according to the footing diameters (0.33D, 0.67D and 1.00D).

3. Test results and discussion

3.1. Series I tests: tests on natural clay deposit

In the Series I tests, a total of seven in situ tests were conducted with seven different circular foundations (diameters of 0.06, 0.09, 0.12, 0.30, 0.45, 0.60 and 0.90 m) resting on the natural clay deposit. Load–settlement curves for all sizes are presented in Fig. 6. The horizontal and vertical axes show the load and settlement ratios, respectively. As can be seen in the figure, the bearing capacity increased with an increase in the foundation size. Bearing

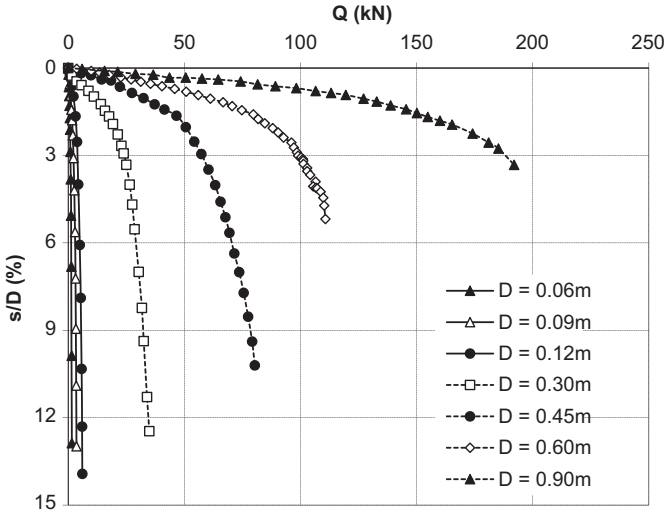


Fig. 6. Curves of load against settlement in Series I tests.

Author's personal copy

capacities of approximately 190 kN and 1.0 kN were obtained for diameters of 0.90 m and 0.06 m, respectively. These values were derived at the settlement ratio of 3%. The settlement ratio of 3% was obtained for all of the footing sizes. For $D=0.90$ m, the natural clay soil deposit collapsed and there was no longer load applied after $s/D>3\%$. Therefore, $s/D=3\%$ is used for all the footing sizes in order to discuss improvements in the bearing capacity. Since the load was applied directly through the natural clay soil in the Series I tests, the settlement pattern generally resembles a typical punching-shear failure.

3.2. Series II tests: tests on granular fill layer placed on natural clay deposit

The effect of the granular fill layer thickness on the bearing capacity and the settlement behaviour was investigated in the Series II tests. In the tests, the granular fill thickness was changed depending on the footing diameter as 0.33, 0.67 and 1.00D. The bearing capacity–settlement curves for the typical sizes of $D=0.09$ m and 0.90 m are presented in Fig. 7.

It can be seen from Fig. 7 that the relationship between the bearing capacity (q)–settlement ratios (s/D) for all the curves is fairly linear for small-load ranges, and that the relationship is nonlinear for large-load ranges and does not exhibit any peak values. Also, from a comparison of the curves for different H/D values, it can be seen that the load–settlement behaviour became stiffer as the H/D ratio increased, due to partially replacing the natural clay soil with a layer of compacted stiffer granular fill, for both $D=0.09$ m and 0.90 m footing diameters. In the Series II tests, the bearing capacity is a function of H/D (Madhav and Vitkar, 1978; Hamed et al., 1986).

The contributions of granular fill layers on the bearing capacity are presented by the term Bearing Capacity Ratio (BCR). The term BCR is commonly used to express and compare the test data on reinforced and unreinforced soils. The following well-established definition (Binquet and Lee, 1975a) is used for BCR:

$$\mathrm{BCR}=q_R/q_0 \tag{1}$$

where q_R and q_0 are the bearing capacity for the reinforced (granular fill layer placed on natural clay deposit) and unreinforced (natural clay deposit) soils, respectively. The parameters investigated, including the settlement of footing plate, s, are normalised by the diameter of the footing plate, D (Laman and Yildiz, 2003). The bearing capacity obtained at $s/D=3\%$ is used to calculate the corresponding BCRs. The settlement ratio (s/D) is defined as the ratio of the footing settlement (s) to the footing diameter (D).

Fig. 8 shows the relation of BCR to the H/D ratio obtained from the Series II tests using the values of the bearing capacity evaluated by Eq. (1). H/D is defined as the ratio of the granular fill thickness (H) to the footing diameter (D). It is shown that the bearing capacity of all the circular footings increased when partially replacing the natural clay soil with the compacted stiffer granular fill

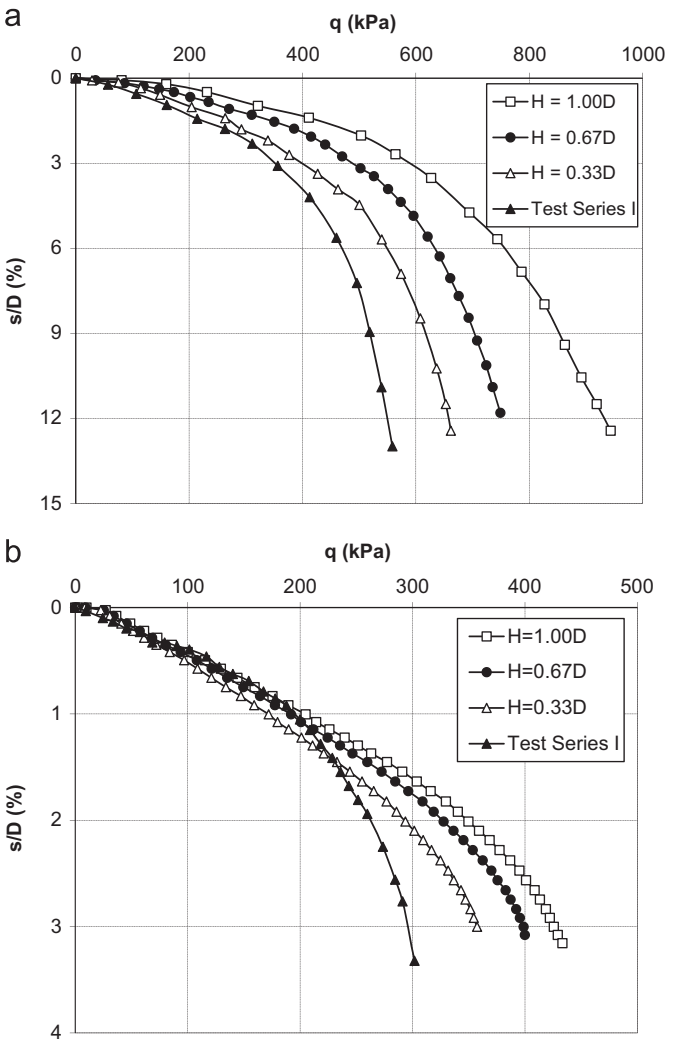


Fig. 7. Bearing capacity–settlement curves in Series II tests. (a) D=0.09 m and (b) =0.9 m.

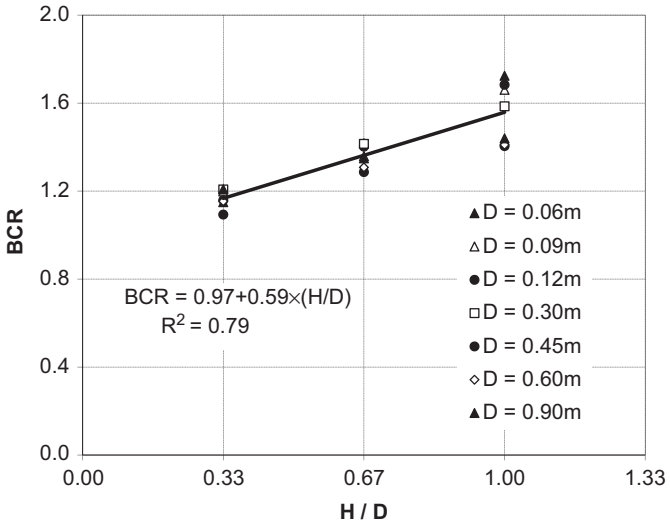


Fig. 8. BCR relations in Series II tests.

Author's personal copy

layer, and also that BCR increased with an increase in the granular fill thickness for all footing diameters. The BCR values obtained for $D=0.90$ m are 1.21, 1.35 and 1.44 for $H=0.33D$; $H=0.67D$ and $H=1.00D$, respectively. Seven different sets of data were used in Fig. 8 for different diameters of footings. The data are close to each other, except for the results of $H/D=1.00$, which are slightly different, so that a simple best fit line with an R^2 of 0.79 was obtained from the regression analysis.

4. Overview of artificial neural networks

Artificial neural networks are a form of artificial intelligence, which by means of their architecture, try to simulate the behaviour of the human brain and nervous system. They have the ability to relate input data and corresponding output data, which can be defined depending on single or multiple parameters for solving linear or nonlinear problems. Artificial neural networks do not require any prior knowledge or a physical model of the problem to solve it. The nature of the relationship between the input and the output parameters is captured by means of learning the samples in the data set (Shahin et al., 2001; Juang et al., 2001). Artificial neural networks can be applied successfully to solve problems which have no specific solutions and are too complex to be modelled mathematically or with traditional methods (Thirumalaiah and Deo, 1998; Adeli, 2001). A comprehensive description of ANNs can be found in many publications (e.g., Hecht-Nielsen, 1990; Zurada, 1992; Maier and Dandy, 2000; Shahin et al., 2001).

In this study, the artificial neural network approach, namely, multi-layer perceptron (MLP) and multi-linear regression (MLR) models were used. The results of the field studies were compared with those obtained by the MLP and MLR approaches.

An MLP distinguishes itself by the presence of one or more hidden layers, whose computation nodes are correspondingly called the hidden neurons of hidden units. An MLP network structure is shown in Fig. 9. The function of the hidden neurons is to intervene between the external input and the network output in some useful manner. The number of hidden layer neurons is found by performing a simple trial-and-error method in all applications. The sigmoid and linear functions are used for the activation functions of the hidden and output nodes, respectively.

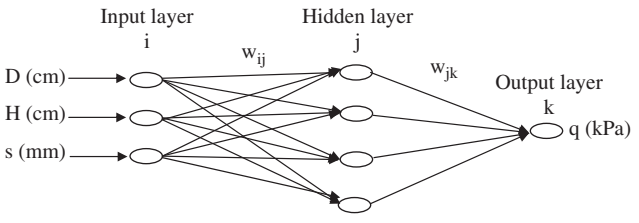


Fig. 9. Chosen model architecture.

Detailed theoretical information about MLPs can be found by Haykin (1998). Here, the MLP is trained using the Levenberg–Marquardt technique, because this technique is more powerful and faster than the conventional gradient descent technique (Hagan and Menhaj, 1994; El-Bakyr, 2003).

A typical structure of artificial neural networks consists of a number of processing elements, or nodes, which are usually arranged in layers, namely, an input layer, an output layer and one or more hidden layers (Fig. 9) (Haykin, 1998).

Each processing element in a specific layer is fully or partially joined to many other processing elements via weighted connections. The input from each element in the previous layer (x_i) is multiplied by an adjustable connection weight (w_{ji}). At each element, the weighted input signals are summed and a threshold value or bias (θ_j) is added. This combined input (I_j) is then passed through a nonlinear transfer function ($f(.)$) (e.g., sigmoidal transfer function and tanh transfer function) to produce the output of the processing elements (y_j). The output of one processing element provides the input to the processing elements in the next layer. This process is summarised in Eqs. (2) and (3) and illustrated in Fig. 9:

$$I_j = \sum w_{ji}x_i + q_j \qquad \text{summation} \tag{2}$$

$$y_j = f(I_j) \qquad \text{transfer} \tag{3}$$

The propagation of information in the artificial neural networks starts at the input layer where the network is presented with a historical set of input data and the corresponding (desired) outputs. The actual output of the network is compared to the desired output and an error is calculated. Using this error and utilising a learning rule, the network adjusts its weights until it can find a set of weights that will produce the input/output mapping that has the smallest possible error. This process is called "learning" or "training". It should be noted that a network with one hidden layer can approximate any continuous function provided that sufficient connection weights are used (Cybenko, 1989; Hornik et al., 1989). The objective of the learning is to capture the relationship between the input and the output parameters. For this purpose, network models are trained using a learning algorithm. Here, the MLP is trained using the Levenberg–Marquardt (LM) learning algorithm due to fact that this technique is more powerful and faster than the conventional gradient descent technique (Hagan and Menhaj, 1994; El-Bakyr, 2003; Cigizoglu and Kisi, 2005). The Levenberg–Marquardt algorithm is an approximation of Newton's method, and Hagan and Menhaj (1994) showed that it is very efficient for training networks which have up to a few hundred weights. Although the computational load of the Levenberg–Marquardt algorithm is greater than the other techniques, this is compensated by the increased efficiency and much better precision in the results. In many cases, the Marquardt algorithm was

Author's personal copy

found to converge when other back-propagation techniques diverged (Hagan and Menhaj, 1994). If there is a function, $V(\underline{x})$, which is to be minimised with respect to the parameter vector, $\underline{x}$, then Newton's method would be

$$\Delta x = -[\nabla^2 V(x)]^{-1} \nabla V(x) \tag{4}$$

where $\nabla^2 V(\underline{x})$ is the Hessian matrix and $\nabla V(\underline{x})$ is the gradient. If we assume that $V(\underline{x})$ is a sum of squares function,

$$V(\underline{x}) = \sum_{i=1}^{N} e_i^2(\underline{x}) \tag{5}$$

then it can be shown that

$$\nabla V(\underline{x}) = J^T(\underline{x}) e(\underline{x}) \tag{6}$$

$$\nabla^2 V(\underline{x}) = J^T(\underline{x}) J(\underline{x}) + S(\underline{x}) \tag{7}$$

where $J(\underline{x})$ is the Jacobean matrix and $S(\underline{x})$ is described as follows:

$$S(\underline{x}) = \sum_{i=1}^{N} e_i \nabla^2 e_i(\underline{x}) \tag{8}$$

For the Gauss–Newton method, it is assumed that $S(\underline{x}) \approx 0$, and the update of Eq. (4) becomes

$$\Delta \underline{x} = [J^T(\underline{x}) J(\underline{x})]^{-1} J^T(\underline{x}) e(\underline{x}) \tag{9}$$

The Levenberg–Marquardt modification to the Gauss–Newton method is

$$\Delta \underline{x} = [J^T(\underline{x}) J(\underline{x}) + \mu I]^{-1} J^T(\underline{x}) e(\underline{x}) \tag{10}$$

Parameter μ is multiplied by a β factor whenever a step would result in an increased $V(\underline{x})$. When a step reduces $V(\underline{x})$, μ is divided by β. When μ is large, the algorithm becomes the steepest descent (with step $1/\mu$), while for small μ, the algorithm becomes the Gauss–Newton. The Levenberg–Marquardt algorithm can be considered a trust-region modification to the Gauss–Newton. The key step in this algorithm is the computation of the Jacobean matrix. For neural network-mapping problems, the terms in the Jacobean matrix can be computed by a simple modification to the back-propagation algorithm (Mamak et al., 2009).

The great majority of the civil engineering applications of neural networks are based on the use of the back-propagation (BP) algorithm, primarily because of its simplicity (Laman and Uncuoglu, 2009). In the BP algorithm, training is supervised such that the network connection weights are adjusted according to the sum of the squares of the differences between the actual and the target outputs.

The goal of the training is to reduce the error function iteratively, defined in the form of the sum of the squares of the errors between the actual outputs and the target outputs. Global error, E, can be defined as

$$E = \frac{1}{p} \sum_{p=1}^{p} E_p \tag{11}$$

where p is the total number of training samples and E_p is the error for training sample$p$.

E_p is calculated by the following equation:

$$E_p = \frac{1}{2} \sum_{i=1}^{N} (o_i - t_i)^2 \tag{12}$$

In this equation, N, o_i and t_i represent the total number of output neurons, the network output at the ith output neuron and the target output at the ith output neuron, respectively (Maier and Dandy, 2000; Shahin et al., 2001). The information related to the theory and the applications of ANNs may be found by Rumelhart and McClelland (1986).

5. Artificial neural network application

In this study, artificial neural networks were used to predict the bearing capacity of circular shallow footings supported by layers of compacted granular fill over natural clay soil. For this purpose, multilayer feed forward network models have been trained using an LM learning algorithm. The data used to run the network models have been obtained from the above-mentioned field tests. Details of the field tests are given in Sections 2 and 3.

The problem is proposed to network models by means of three input parameters representing the diameter of the footing (D), the thickness of the granular fill layer (H), the settlement of the footing (s) and one output parameter representing the bearing capacity (q).

It is common practice to split the available data into two sub-sets, namely, a training set and an independent validation set (Maier and Dandy, 2000). The literature offers little guidance when selecting the size of the training and the test samples. Most authors select the ratio of the training data and the testing data depending on the particular problem (Kisi, 2005; Sudheer, 2005; Dogan et al., 2008). Thus, a total of 751 individual data samples, obtained from experimental studies, were used for the training and the testing of the network models. The available data set were divided into two groups, training and testing data sets, which consisted of 512 and 239 data samples, respectively. The data samples were selected randomly from the available data set to constitute the mentioned data sets. One important aspect here is to make sure that the minimum and the maximum testing data set fall within the minimum and the maximum training data set. The statistical properties and the range in parameters are shown in Tables 1 and 2, respectively. In Table 1, parameters, X_{min}, X_{max}, X_{mean}, S_x and C_{sx} refer to the minimum value, the maximum value, the mean value, the standard deviation value and the skewness coefficient of the training and the testing data sets, respectively.

To develop the best network model, given the available data set, the training data set should contain all representative samples that are present in the available data set (Shahin et al., 2004). As seen in Table 1, the data sets represent the same problem domain such that the

Author's personal copy

Table 1
Statistical properties of data sets.

	X_{min}	X_{max}	X_{mean}	S_x	C_{sx}
Training data set					
D (m)	0.06	0.90	0.48	0.31	−0.01
H (m)	0	0.90	0.19	0.24	1.16
s (m)	0	0.053	0.012	0.01	1.16
q (kPa)	0	948.16	351.17	212.55	0.27
Test data set					
D (m)	0.06	0.90	0.42	0.28	0.55
H (m)	0	0.90	0.28	0.28	1.18
s (m)	0	0.047	0.012	0.01	1.08
q_u (kPa)	0	856.18	350.80	202.88	0.08

Table 2
Ranges of parameters.

Model variable	Minimum value	Maximum value	Range
D (m)	0	0.90	0.90
H (m)	0	0.90	0.90
s (m)	0	0.053	0.053
q (kPa)	0	948.16	948.16

statistical properties of the data sets are consistent with each other. In any model development process, familiarity with the available data is of the utmost importance. In general, different variables span different ranges. In order to ensure that all variables receive equal attention during the training process, they should be standardized.

Preprocessing of the data is usually required before presenting the data samples to the network model when the neurons have a transfer function with bounded range. The reasons for scaling the data samples are to initially equalise the importance of the variables and to improve the interpretability of the network weights (Goh, 1995).

Determining an appropriate architecture of the neural network for a particular problem is an important issue, since the network topology directly affects its computational complexity and generalisation capability (Kisi and Uncuoglu, 2005). Multilayer feed forward network models with one hidden layer can approximate any complex nonlinear function provided a sufficient number of hidden layer neurons is available. In this study, therefore, multilayer feed forward network models containing one hidden layer were used.

Determining the optimum number of hidden layer neurons is very important for accurately predicting a parameter using artificial neural networks. However, there is no theory for how many hidden layer neurons need to be used for a particular problem. For that reason, the numbers of hidden layer neurons have generally been determined by a trial-and-error method. A common strategy for finding the optimum number of hidden layer neurons is to start with a few neurons and to increase the number of neurons, while monitoring the performance criteria, until no significant improvement is observed (Goh, 1995; Nawari et al., 1999).

In this study, the performance of various network models with different numbers of hidden layer neurons was examined in order to choose an appropriate number of hidden layer neurons. Hence, two neurons were used in the hidden layer at the beginning of the process, and then the number was increased step-by-step adding one neuron until no significant improvement was noted.

The MLR technique was applied to both the testing and the training data sets. The following formulas, using the MLR technique, were found to offer the best fitting statistical measures for the testing and training data sets, respectively:

$$q = 83.5D - 30H + 20243s \tag{13}$$

$$q = 28.1D + 118H + 17012s \tag{14}$$

where q (kPa) is the bearing capacity, s (m) is the footing settlement, H (m) is the granular fill thickness and D (m) is the footing diameter.

The network models were tried and compared according to mean absolute relative error (MARE) and mean square error (MSE) criteria. These criteria are defined as

$$\mathrm{MARE} = \frac{1}{N}\sum_{i=1}^{N}\frac{\left|M_{i_{measured}} - M_{i_{predicted}}\right|}{M_{i_{measured}}} \times 100 \tag{15}$$

$$\mathrm{MSE} = \frac{\sum_{i=1}^{N}\left(M_{i_{measured}} - M_{i_{predicted}}\right)^2}{N} \tag{16}$$

In these equations, N and M denote the total number of data samples and bearing capacities, respectively.

At the end of these processes, the best performance was obtained from the ANN model which has four neurons in the hidden layer. The chosen model architecture is shown in Fig. 9.

The training of the network models is carried out by presenting the training data set involving pairs of input–output data. The connection weights are adjusted during the training phase according to the differences between the target output ($M_{measured}$) and the actual output ($M_{predicted}$) (Kisi and Uncuoglu, 2005).

Author's personal copy

Table 3
Saved weights from input layer to hidden layer.

Neuron number	I_1	I_2	I_3
H_1	0.872	−0.337	−2.339
H_2	−4.547	3.023	−27.511
H_3	11.138	−8.745	−0.824
H_4	8.427	−4.058	−7.270

Table 4
Saved weights from hidden layer to output layer.

Neuron number	H_1	H_2	H_3	H_4
O_1	−2.3217	−6.0613	−5.2341	0.0767

Table 5
Saved bias values.

Neuron number	Bias value
H_1	−1.2103
H_2	4.0043
H_3	1.8147
H_4	−3.3966
O_1	−2.5091

The adjustment of the connection weights is continued until the mean square error over all the training samples falls below a given value or the maximum number of epoch is reached. In the training phase, the performance of the network models is monitored at each epoch using the test data set. In this way, the overfitting of the network model can be prevented. When the training phase was complete, the weights were saved for use in the test phase. The saved weights and bias values used in the chosen network model with four hidden layer neurons are presented in Tables 3–5.

To compare the results obtained from the network and the regression models with the experimental results, the predicted values were transformed back to their original values and then MARE and MSE were computed.

The tangent sigmoid, logarithmic sigmoid and pure linear transfer functions were tried as activation functions for the hidden and the output layer neurons to determine the best network model (Haykin, 1998). The most appropriate results have been obtained from the chosen network model in which the tangent sigmoid and the pure linear functions were used as the activation function for the hidden and the output layer neurons, respectively. The programme used in running the network models was written in Matlab language code.

The MSE (mean square error), MARE (mean absolute relative error) and R^2 (determination coefficient) values of MLP and MLR, for both training and testing phases, are given in Table 6.

As seen from Table 6, the MLP model has the smaller MSE (501.081) and MARE (11.343) values and the higher R^2 (0.988) value for the training phase. It also has the smaller MSE (1670.661) and MARE (18.420) values and the higher R^2 (0.950) value for the testing phase. According to the statistical analyses, the MLP estimations are better

Table 6
Results obtained from chosen network model and regression model.

	MLP	**MLR**
Train MSE (kPa)	501.081	69,133.740
Test MSE (kPa)	1670.661	56,996.477
Train MARE	11.343	51.282
Test MARE	18.420	47.052
R^2_{train}	0.988	0.480
R^2_{test}	0.950	0.249
Epoch number	63	–
Hidden layer neurons	4	–

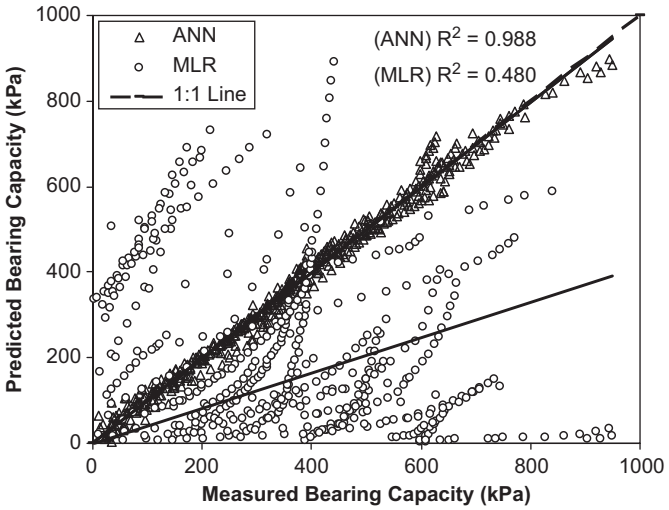


Fig. 10. Correlation between measured and predicted bearing capacities in training phase.

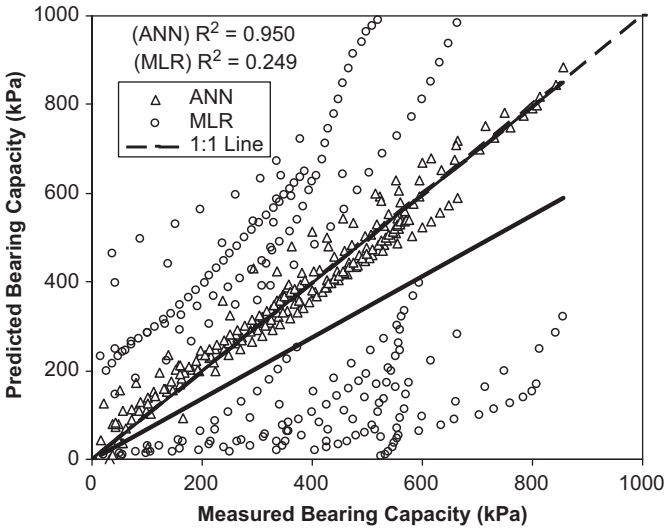


Fig. 11. Correlation between measured and predicted bearing capacities in testing phase.

Author's personal copy

than those of MLR; they also produce more accurate results than MLR. It can be seen from Table 6 that the ANN method performs better than MLR in both the training and the testing phases. In other words, the neural network is able to successfully model the bearing capacity of shallow footings resting on clay soil.

Figs. 10 and 11 present the measured bearing capacities versus the predicted bearing capacities by the network model with R^2 coefficients for the training and the testing phases, respectively. The linear 1:1 lines were also plotted in these figures to discuss the performance of the statistical models. It is seen from the figures that for the artificial neural network (ANN) model approach, the location points of the measured and the predicted bearing capacity values are scattered around the 1:1 lines for both training and testing phases. On the other hand, the multi-linear regression model gives results in a broad band, especially in the training phase. The prediction performance increases from 48.0% to 98.8% for the training phase and from 24.9% to 95.0% for the testing phase, when the determination coefficients (R^2) were considered. It is concluded that a statistical model based on the artificial neural network approach, namely, MLP, is also proposed as an alternative to the MLR technique. MLP produced more accurate results than the MLR technique.

6. Conclusions

In this study, field tests were performed using seven different footing diameters, up to 0.90 m, and three different granular fill layer thicknesses. At the end of the tests, load–settlement curves were plotted, and artificial neural networks (ANNs) and the multi-linear regression model (MLR) were used to predict the bearing capacity of circular shallow footings supported by a compacted granular fill layers over natural clay soil. Based on the results of this investigation, the following main conclusions can be drawn:

- It has been observed from the unreinforced field test results that the bearing capacity increased with an increase in foundation size. Bearing capacities of approximately 190 kN and 1.0 kN were obtained for diameters of 0.90 m and 0.06 m, respectively. The settlement pattern generally resembled a typical punching-shear failure under natural clay soil conditions.
- The field test results have indicated that the use of granular fill layers over natural clay soil has a considerable effect on the bearing capacity and the settlement characteristics.
- In the tests, the granular fill thickness (H) was changed depending on the footing diameter as 0.33, 0.67 and 1.00D. The bearing capacity ratio (BCR) was seen to increase with an increase in the granular fill thickness for all footing diameters. The BCR values for $D=0.90$ m obtained are 1.21, 1.35 and 1.44 for $H=0.33D$; $H=0.67D$ and $H=1.00D$, respectively.
- A neural network model has been also developed for this problem. The input parameters for assessing the bearing capacity of shallow footings by ANNs are the diameter of the footing (D), the thickness of the granular fill layer (H) and the settlement of the footing (s). The output of the neural network is the predicted bearing capacity of the shallow footings in natural clay deposits.
- The artificial neural network model serves as a simple and reliable tool for the bearing capacity of circular footings in natural clay soil stabilized with granular fill. The results produced high coefficients of correlation for the training and testing data of 0.988 and 0.950, respectively.
- A statistical model based on the artificial neural network approach, namely MLP, was also proposed as an alternative to the MLR technique. MLP produced more accurate results than the MLR technique, and MLP gave better results between them in terms of MSE ($=501.081$), MARE ($=11.343\%$) and R^2 ($=0.988$) statistics.

Nevertheless, this investigation is considered to have provided a useful basis for further research leading to an increased understanding of the application of soil reinforcement to ultimate bearing capacity problems.

Acknowledgements

The work presented in this paper was carried out with funding from TUBITAK (Scientific and Technological Research Council of Turkey), Grant no. 106M496, and the Cukurova University Scientific Research Project Directorate, Grant no. MMF2006D28.

References

Abu-Farsakh, M., Chen, Q., Sharma, R., Zhang, X., 2008. Large scale model footing tests on geogrid reinforced footing and marginal embankment soils. Geotechnical Testing Journal 31 (5), 413–423.

Adams, M., Collin, J., 1997. Large model spread footing load tests on geosynthetic reinforced soil footings. Journal of Geotechnical and Geoenvironmental Engineering 123 (1), 66–72.

Adeli, H., 2001. Neural networks in civil engineering 1989–2000. Computer-Aided Civil and Infrastructure Engineering 16, 126–142.

Alawaji, H.A., 2001. Settlement and bearing capacity of geogrid-reinforced sand over collapsible soil. Geotextiles and Geomembranes 19, 75–88.

ASTM, 1997. Standard test method for nonrepetitive static plate load tests of soils and flexible pavement components, for use in evaluation and design of airport and highway pavements. pp. 112–113.

Basma, A.A., Kallas, N., 2004. Modelling soil collapse by artificial neural networks. Geotechnical and Geological Engineering 22, 427–438.

Binquet, J., Lee, K.L., 1975a. Bearing capacity tests on reinforced earth slabs. Journal of the Geotechnical Engineering Division—ASCE 101 (GT12), 1241–1255.

Chen, Q., 2007. An Experimental Study on Characteristics and Behavior of Reinforced Soil Footing. Ph.D. Thesis. Louisiana State University, Baton Rouge, USA.

Cho, S.E., 2009. Probabilistic stability analyses of slopes using the ANN-based response surface. Computers and Geotechnics 36 (5), 787–797.

Author's personal copy

Cobaner, M., Haktanir, T., Kisi, O., 2008. Prediction of hydropower energy using ANN for the feasibility of hydropower plant installation to an existing irrigation dam. Water Resources Management 22 (6), 757–774.

Cybenko, G., 1989. Approximation by superpositions of a sigmoidal function. Mathematics of Control, Signals, and Systems 3, 303–314.

Dash, S.K., Sireesh, S., Sitharam, T.G., 2003. Model studies on circular footing supported on geocell reinforced sand underlain by soft clay. Geotextiles and Geomembranes 21, 197–219.

Deb, K., Sivakugan, N., Chandra, S., Basudhar, P.K., 2007. Numerical analysis of multi layer geosynthetic-reinforced granular bed over soft fills. Geotechnical and Geological Engineering 25, 639–646.

Dogan, A., Demirpence, H., Cobaner, M., 2008. Prediction of groundwater levels from lake levels and climate data using ANN approach. Water SA 34 (2), 199–208.

El-Bakyr, M.Y., 2003. Feed forward neural networks modelling for k–p interactions. Chaos, Solitons and Fractals, Elsevier 18 (5), 995–1000.

Fausett, L.V., 1994. Fundamentals Neural Networks: Architecture, Algorithms, and Applications. Prentice-Hall, Englewood Cliffs, New Jersey.

Goh, A.T.C., 1995. Back-propagation neural networks for modelling complex systems. Artificial Intelligence in Engineering vol. 9, 143–151.

Hagan, M.T., Menhaj, M.B., 1994. Training feed forward networks with the Marquardt algorithm. IEEE Transactions on Neural Networks 5 (6), 861–867.

Hamed, J.T., Das, B.M., Echelberger, W.F., 1986. Bearing capacity of a strip foundation on granular trench in soft clay. Civil Engineering for Practising and Design Engineers 5 (5), 359–376 (Paragon Press).

Haykin, S., 1998. Neural Networks—A Comprehensive Foundation 2nd Ed. Prentice-Hall, Upper Saddle River, NJ, pp. 26–32.

Hecht-Nielsen, R., 1990. Neurocomputing. Addison-Wesley Publishing Company, Reading, MA.

Hornik, K., Stinchcombe, M., White, H., 1989. Multilayer feedforward networks are universal approximators. Neural Networks 2, 359–366.

Juang, C.H., Jiang, T., Christopher, R.A., 2001. Three-dimensional site characterization: neural network approach. Geotechnique 51 (9), 799–809.

Kayadelen, C., 2008. Estimation of effective stress parameter of unsaturated soils by using artificial neural networks. International Journal for Numerical and Analytical Methods in Geomechanics 32 (9), 1087–1106.

Kisi, O., 2005. Suspended sediment estimation using neuro-fuzzy and neural network approaches. Hydrologıcal Scıences Bulletın 50 (4), 683–696.

Kisi, O., Uncuoglu, E., 2005. Comparison of three back-propagation training algorithms for two case studies. Indian Journal of Engineering and Material Sciences 12, 434–442.

Kung, G.T.C., Hsiao, E.C.L., Schuster, M., Juang, C.H., 2007. A neural network approach to estimating deflection of diaphragm walls caused by excavation in clays. Computers and Geotechnics 34 (5), 385–396.

Kuo, Y.L., Jaksa, M.B., Lyamin, A.V., Kaggwa, W.S., 2009. ANN-based model for predicting the bearing capacity of strip footing on multilayered cohesive soil. Computers and Geotechnics 36 (3), 503–516.

Laman, M., Yildiz, A., 2003. Model studies of ring footings on geogrid-reinforced sand. Geosynthetics International 10 (5), 142–152.

Laman, M., Yildiz, A., Ornek, M., Demir, A., 2009. Geogrid reinforcement on soft clay deposit. TUBITAK Scientific Research Project (no. 106M496), Ankara, Turkey, 528 pp.

Laman, M., Uncuoglu, E., 2009. Prediction of the moment capacity of short pier foundations in clay using the neural networks. Kuwait Journal of Science and Engineering 36 (1B), 1–20.

Madhav, M.R., Vitkar, P.P., 1978. Strip footing on weak clay stabilized with a granular trench or pile. Canadian Geotechnical Journal 15 (4), 605–609.

Maier, H.R., Dandy, G.C., 2000. Applications of artificial neural networks to forecasting of surface water quality variables: issues, applications and challenges. In: Govindaraju, R.S., Rao, A.R. (Eds.), Artificial Neural Networks in Hydrology. Kluwer, Dordrecht, The Netherlands, pp. 287–309.

Mamak, M., Seckin, G., Cobaner, M., Kisi, O., 2009. Bridge afflux analysis through arched bridge constrictions using artificial intelligence methods. Civil Engineering and Environmental Systems 26 (3), 279–293.

Nawari, N.O., Liang, R., Nusairat, J., 1999. Artificial intelligence techniques for the design and analysis of deep foundations. Electronic Journal of Geotechnical Engineering 〈http://www.ejge.com/1999/Ppr9909/Ppr9909.htm〉.

Ochiai, H., Watari, Y., Tsukamoto, Y., 1996. Soil reinforcement practice for fills over soft ground in Japan. Geosynthetics International 3 (1), 31–48.

Ornek, M., 2009. Geogrid Reinforcement on Soft Clay Deposits. Ph.D. Thesis, University of Cukurova, Turkey, 318 pp. (in Turkish).

Otani, J., Ochiai, H., Yamamoto, K., 1998. Bearing capacity analysis of reinforced foundations on cohesive soil. Geotextiles and Geomembranes 16, 195–206.

Padmini, D., Ilamparuthi, K., Sudheer, K.P., 2008. Ultimate bearing capacity prediction of shallow foundations on cohesionless soils using neurofuzzy models. Computers and Geotechnics 35 (1), 33–46.

Rumelhart, D.E., McClelland, J.L., and The PDP Research Group, 1986. Parallel distributed processing. In: Proceedings: Explorations in the Microstructure of Cognition—Foundations, vol. 1. MIT Press, Bradford Books, Cambridge, MA.

Samui, P., 2010. Application of statistical learning algorithms to ultimate bearing capacity of shallow foundation on cohesionless soil. International Journal for Numerical and Analytical Methods in Geomechanics Available from: www.onlinelibrary.wiley.com/doi/10.1002/nag.997.

Shahin, M.A., Jaksa, M.B., Maier, H.R., 2001. Artificial neural network applications in geotechnical engineering. Australian Geomechanics, 49–62.

Shahin, M.A., Maier, H.R., Jaksa, M.B., 2004. Data division for developing neural networks applied to geotechnical engineering. Journal of Computing in Civil Engineering 18 (2), 105–114.

Sudheer, K.P., 2005. Knowledge extraction from trained neural network river flow models. Journal of Hydrologic Engineering—ASCE 10 (4), 264–269.

Thirumalaiah, K., Deo, M.C., 1998. River stage forecasting using artificial neural networks. Journal of Hydrologic Engineering—ASCE 3 (1), 26–32.

Thome, A., Donato, M., Consoli, N.C., Graham, J., 2005. Circular footings on a cemented layer above weak foundation soil. Canadian Geotechnical Journal 42, 1569–1584.

Wang, J., Rahman, M.S., 1999. A neural network model for liquefaction-induced horizontal ground displacement. Soil Dynamics and Earthquake Engineering 18 (8), 555–568.

Yin, J.H., 1997. Modeling geosynthetic-reinforced granular fills over soft soil. Geosynthetics International 4 (2), 165–185.

Zurada, J.M., 1992. Introduction to Artificial Neural Systems. West Publishing Company, St. Paul.